AIP | Applied Physics Letters

High efficiency mesoporous titanium oxide PbS quantum dot solar cells at low temperature

Tong Ju, Rebekah L. Graham, Guangmei Zhai, Yvonne W. Rodriguez, Alison J. Breeze, Lily Yang, Glenn B. Alers, and Sue A. Carter

Citation: Applied Physics Letters **97**, 043106 (2010); doi: 10.1063/1.3459146
View online: http://dx.doi.org/10.1063/1.3459146
View Table of Contents: http://scitation.aip.org/content/aip/journal/apl/97/4?ver=pdfcov
Published by the AIP Publishing

Articles you may be interested in

Enhancement of the photovoltaic performance in P3HT: PbS hybrid solar cells using small size PbS quantum dots
J. Appl. Phys. **116**, 094305 (2014); 10.1063/1.4894404

Increased open-circuit voltage in a Schottky device using PbS quantum dots with extreme confinement
Appl. Phys. Lett. **102**, 193902 (2013); 10.1063/1.4804614

PbS nanocrystal solar cells with high efficiency and fill factor
Appl. Phys. Lett. **97**, 203501 (2010); 10.1063/1.3518067

Viability of using near infrared PbS quantum dots as active materials in luminescent solar concentrators
Appl. Phys. Lett. **96**, 191901 (2010); 10.1063/1.3422485

Near-IR activity of hybrid solar cells: Enhancement of efficiency by dissociating excitons generated in PbS nanoparticles
Appl. Phys. Lett. **96**, 073505 (2010); 10.1063/1.3292183

AIP | Applied Physics Letters
Meet The New Deputy Editors

Alexander A. Balandin

Qing Hu

David L. Price

This article is copyrighted as indicated in the article. Reuse of AIP content is subject to the terms at: http://scitation.aip.org/termsconditions. Downloaded to IP: 128.114.130.190 On: Fri, 30 Jan 2015 21:49:13

High efficiency mesoporous titanium oxide PbS quantum dot solar cells at low temperature

Tong Ju,[1] Rebekah L. Graham,[1] Guangmei Zhai,[2] Yvonne W. Rodriguez,[1] Alison J. Breeze,[3] Lily Yang,[1] Glenn B. Alers,[1,a)] and Sue A. Carter[1,b)]
[1]*Department of Physics, University of California, Santa Cruz, California 95064, USA*
[2]*Huazhong University of Science and Technology, Wuhan, Hubei 430074, People's Republic of China*
[3]*Solexant Corporation, San Jose, California 95131, USA*

(Received 7 April 2010; accepted 11 June 2010; published online 28 July 2010)

Efficient charge transport is demonstrated in TiO_2/PbS quantum dot solar cells where the PbS absorber (~1.1 eV band gap) is deposited by dip coating and ethanedithiol ligand exchange, with power efficiencies above 3% at AM1.5. An increase in power efficiency occurs as the device temperature is lowered to 170 K, with a open-circuit voltage of 0.66 V, short-circuit current density of 28.6 mA/cm^2 and fill factor of 42.4%. This remarkable temperature dependence is due to a large increase in charge transport between the PbS quantum dots with decreasing temperature. © *2010 American Institute of Physics*. [doi:10.1063/1.3459146]

The discovery of high efficiency multiple exciton generation in colloidal PbSe and PbS quantum dot solutions[1,2] has led to substantial research into quantum dot solar cells that can exploit these properties. PbS quantum dots are also considered as an encouraging candidate in tandem cells because their tunable optical band gap (0.4 up to 1.5 eV) enhances infrared absorption.[3] In the past several years, Schottky solar cells composed of nanoparticle PbS and/or PbSe quantum dot thin films have been reported[4–7] with power efficiencies exceeding 3%. In attempts to improve absorption in the ultrathin films, charge extraction and device performance of PbS and PbSe quantum dot solar cells on ZnO nanoparticles and nanorod surfaces have also been studied.[8,9] Several groups have also reported photocurrent studies of PbS quantum dots in porous TiO_2 films[3,10,11] and devices consisting of TiO_2 and PbS films deposited via solution precursor methods.[5,12]

Here, we report efficient charge transfer and extraction in photovoltaic devices consisting of mesoporous TiO_2 and a PbS quantum dot absorber using an air-stable gold (Au) top electrode. The performance of TiO_2/PbS solar cells was influenced by several factors, including TiO_2 particle size, cell thickness, and back contacts, as has been observed for other systems.[13,14] The typical performance of greater than 3% efficiency at AM1.5 and ambient conditions was achieved for a device with 250 nm thick TiO_2 composed of 37 nm TiO_2 nanoparticles and a 150 nm thick PbS layer, using indium tin oxide (ITO) and gold as the electrodes. Furthermore, the power efficiency substantially improved upon cooling due to increased charge transport between PbS quantum dots.

The photovoltaic device structure, energy diagram, and cross-sectional high-resolution scanning electron microscope (HR-SEM) image of absorbing p-type PbS quantum dots on n-type mesoporous TiO_2 are shown in Fig. 1. The colloidal PbS quantum dots were provided by Solexant, the planar TiO_2 was synthesized using the standard procedure described earlier,[15] and the TiO_2 nanoparticle pastes were provided by Solaronix. A ~100 nm layer of planar TiO_2 was coated by the spin-cast technique on a glass substrate prepatterned with ITO to prevent shorting, followed by a spun-cast nanocrystalline anatase-TiO_2-layer. Both planar and nanoparticle TiO_2 layers were sintered at 450 °C for 20 min in air to improve conductivity. Next, a layer of PbS quantum dots was deposited on TiO_2 under nitrogen atmosphere by dip coating between PbS solution in chloroform and hexane mixture and 1,2-ethanedithiol (EDT) in acetonitrile solution.[16] Finally, 100 nm Au was thermally evaporated as the back contact.

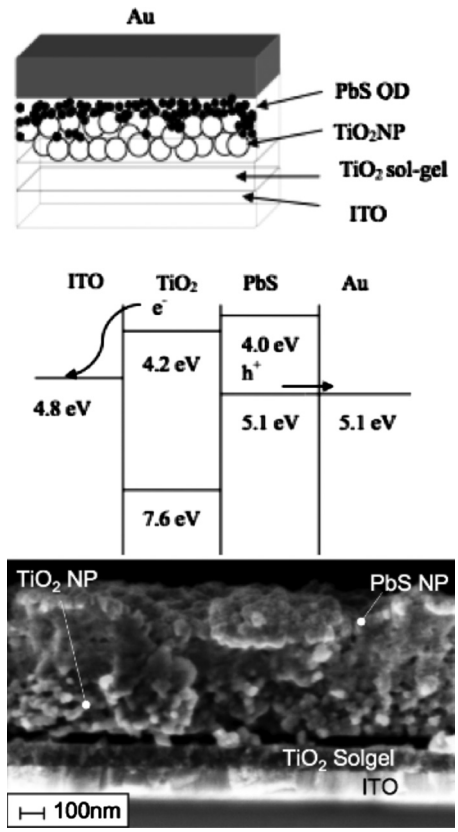

FIG. 1. The schematic sketch (top) of three-dimensional nanocrystalline TiO_2/PbS, where the open circle represents a TiO_2 nanoparticle and solid circle represents a PbS quantum dot; the flat band energy diagram (middle) showing that the electrons are collected by ITO and the holes are collected by Au; and a cross-sectional HR-SEM image (bottom) of the device.

a)Electronic mail: galers@ucsc.edu.
b)Electronic mail: sacarter@ucsc.edu.

 © 2010 American Institute of Physics

This article is copyrighted as indicated in the article. Reuse of AIP content is subject to the terms at: http://scitation.aip.org/termsconditions. Downloaded to IP: 128.114.130.190 On: Fri, 30 Jan 2015 21:49:13

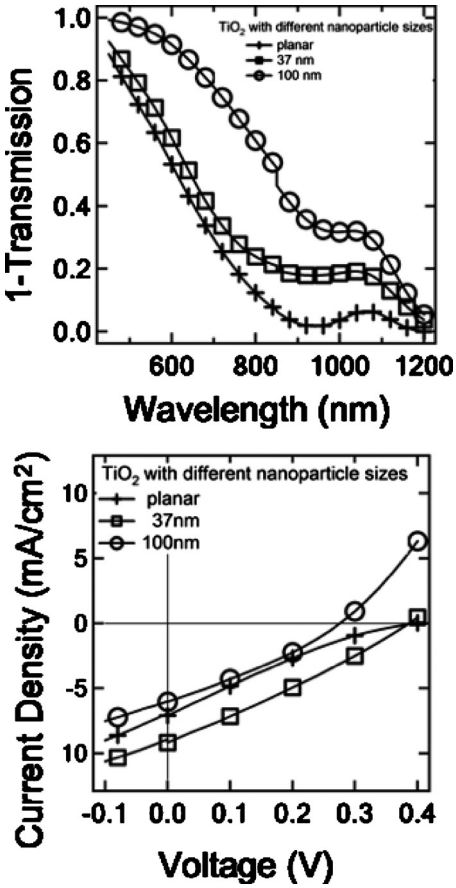

FIG. 2. Transmission (top) of the PbS/TiO_2 films as a function of the TiO_2 nanoparticle size and device performance (bottom) for the same films.

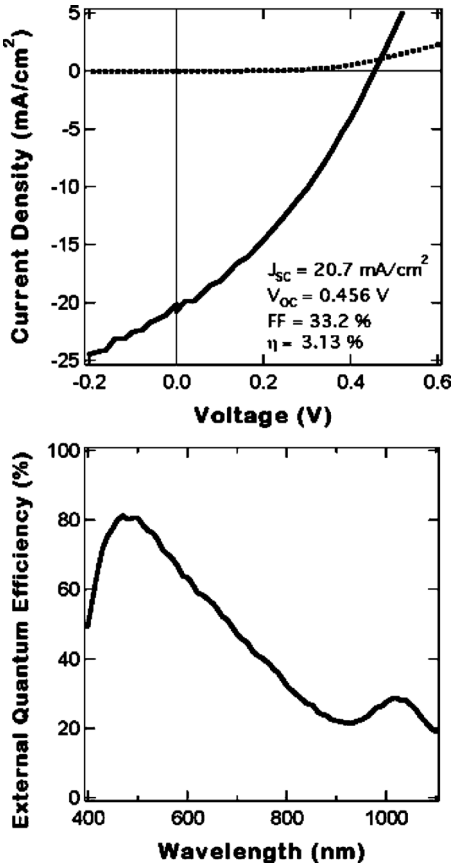

FIG. 3. The J-V curve (top) and EQE (bottom) for a ITO/TiO_2/PbS/Au device, using 37 nm TiO_2 particles and 150 nm thick PbS quantum dot layer.

Current density-voltage (J-V) curves were taken in the dark and under AM1.5 illumination using a calibrated solar simulator. For temperature dependent measurements, a xenon light bulb, placed next to the sample in the cryostat, was used as the light source.

The mesoporous TiO_2 was used to create additional interfacial areas at the TiO_2/PbS surface, compared to the planar structure, in order to improve absorption and charge extraction without sacrificing charge transport. Due to its larger surface area, the device with 100 nm TiO_2 particles has lower transmission (i.e., higher absorption) than both the device with 37 nm TiO_2 particles and the planar device, as shown in Fig. 2. However, the J-V curves reveal that the device with 37 nm TiO_2 particles performs better than the 100 nm particle device. These results suggest that the use of the mesoporous layer detrimentally impacts charge transport in the PbS quantum dot film and that an optimal morphology exists between planar and rougher mesoporous films that balances absorption with charge transport. Surface and device structure morphologies were measured by both HR-SEM (Fig. 1) and an atomic force microscope. While penetration of the PbS into the mesoporous TiO_2 film was observed, it is unlikely that conformal coverage was achieved, which may also limit the performance for larger particle films.

The better performing devices had thicknesses between 120 to 250 nm for PbS, generally consistent with other results on PbS solar cell devices. By varying the preparation conditions of the TiO_2 and the thickness of the PbS layer, power efficiencies above 3% were achieved, as shown in Fig. 3. Under AM1.5, this cell had short-circuit current density (J_{SC}) of 20.7 mA/cm^2, open-circuit voltage (V_{OC}) of 0.456 V, and fill factor (FF) of 33%. External quantum efficiency (EQE) data show significant response in the infrared (IR) and peak EQE was 80% for this device. Moreover, an EQE of nearly 30% was observed even at lower IR energies of $\sim$1.2 eV where the materials were weakly absorbing, suggesting internal quantum efficiencies approaching 100%. We were able to achieve efficient devices made from PbS quantum dots with a $\sim$1.1 eV band gap, in contrast to the 1.3 eV to 1.4 eV band gap typically required for ZnO/PbSe devices,[8] since PbS has a higher electron affinity than PbSe.

The device performance in both light and dark was also studied as a function of temperature (170 to 300 K) in order to understand charge transport. As shown in Fig. 4, a remarkable increase in J_{SC} to 30 mA/cm^2 is observed as the sample is cooled. At 170 K, we observe a J_{SC} of 28.6 mA/cm^2, combined with V_{OC} of 0.66 V and FF of 42.4%. The large increase in J_{SC} is accompanied by over an order of magnitude increase in the dark current, suggesting a large increase in the carrier mobility. These currents are comparable to the best results obtained on PbSe solar cells, and much higher than what has been observed for PbS based devices, implying that the optimal distance between PbS quantum dots is smaller than PbSe. More notable, the V_{OC} of 0.66 V is greater than 0.5 E_g (where $E_g \sim 1.1$ eV), normally considered a limit of Schottky devices. This result suggests that PbS quantum dot solar cells should be able to achieve power efficiencies >8% at room temperature through tuning of the tunneling barrier.

These temperature-dependent results are unexpected because most quantum dot devices undergo Coulomb Blockade

This article is copyrighted as indicated in the article. Reuse of AIP content is subject to the terms at: http://scitation.aip.org/termsconditions. Downloaded to IP: 128.114.130.190 On: Fri, 30 Jan 2015 21:49:13

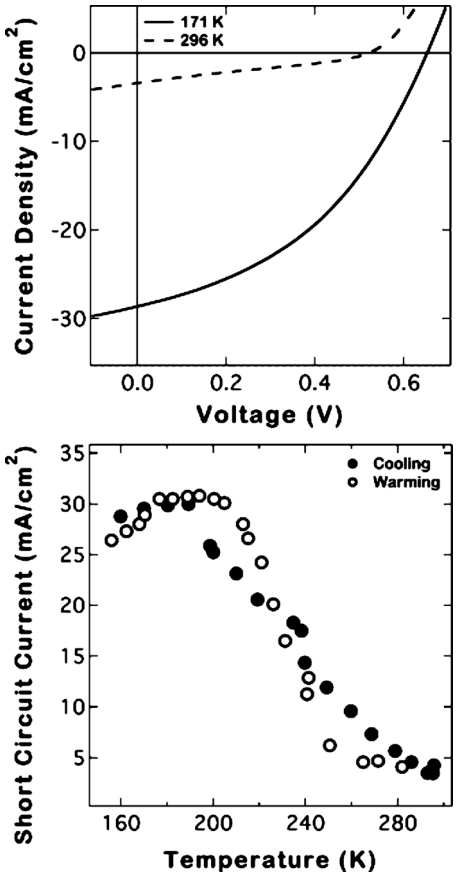

FIG. 4. J-V curves (top) at 296 K and 171 K for an ITO/TiO_2/PbS/Au quantum dot device showing a large improvement in power efficiency (top), and J_{SC} (bottom) with decreasing temperature.

or thermally-activated hopping transport whereby the conductivity decreases with decreasing temperature,[17] as we observe at temperatures below 190 K. An increasing conductivity with decreasing temperature was recently observed for PbSe quantum dot thin films,[18] and attributed to a cross over from tunneling to metallic-like transport. While are devices are clearly not metallic, they are likely dominated by tunneling. Tunneling transport is typically temperature-independent; however, a significant temperature dependence could be caused by thermal contraction of the EDT ligand, which decreases the width of the tunneling barrier and thereby increases the coupling between quantum dots. Recent results by Loef *et al.* of CdSe quantum dot films on TiO_2 support this conclusion.[19] They observe more than an order of magnitude decrease in the transient times, measured by deep level transient spectroscopy, as the samples are cooled from 330 K to 300 K. They are only able to explain their result through thermal contraction of the tunnel barrier due to thermal contraction of the Tri-*n*-octylphosphine oxide (TOPO)/hexadecylamine (HDA) ligand with decreasing temperature. The thermal coefficient for the EDT ligands on our PbS quantum dots is about 2×10^{-4} K^{-1}, resulting in a 5% contraction over the temperature range studied here. The distance between PbS quantum dots, set by the EDT ligand, is about 0.6 nm at 300 K, so this would only result in a 0.03 nm change. However, EDT also has a freezing/melting temperature of −41 C (232 K), near where the peak change in performance is observed, and we note that TOPO has a freezing temperature of ~50 C (323 K) where the large change is observed by Loef *et al.* This freezing of the ligand would further decrease the spacing between particles. Taken together, the effect of the decreased spacing would result in increased mobility, as discussed elsewhere for PbSe quantum dots,[20] which may be sufficient to explain the improvement in J_{SC} from 20 mA/cm^2 (observed in Fig. 3) to the ~30 mA/cm^2 observed at lower temperatures in Fig. 4. Nonetheless, it is insufficient to explain the order of magnitude change that occurs for a single device caused by the lower initial J_{SC} currents. The lower room temperature J_{SC} observed in Fig. 4 is due to the short (~30 min) exposure of the device to oxygen while the sample is loaded into the cryostat. Oxygen exposure of PbS quantum dots is known to cause the EDT ligand to desorb[21] which lowers the J_{SC} by decreasing the coupling between the quantum dots. We hypothesize that the cooling of the film also impacts the ligand absorption/desorption, as others have observed for EDT on nickel between 200 and 300 K,[22] allowing the device to recover its preoxygen exposure performance.

In summary, we have studied the photovoltaic properties of solar cells that use colloidal quantum dot solutions to make TiO_2/PbS heterojunction solar cells with >3% power efficiency. Moreover, we have demonstrated a large increase in device performance as the quantum dot solar cell is cooled. We attribute this effect to enhanced coupling between quantum dots due to thermal contraction and freezing of the organic ligand. Tuning this effect through the selection of alternate ligands provides a promising pathway toward further improving device efficiency at room temperature.

T.J. and S.A.C. acknowledge support through the UC Discovery Program. R.L.G. acknowledges support through the GAANN program. L.Y. acknowledges use of the HRSEM at the Molecular Foundry (DOE Contract No. AC02–05CH11231). G.Z. acknowledges support of China Scholarship Council. GBA and SAC acknowledge support through the DOE SETP program (DOE Grant DE-FC36–08GO18104).

[1]R. J. Ellingson *et al.*, Nano Lett. **5**, 865 (2005).
[2]R. D. Schaller, V. M. Agranovich, and V. I. Klimov, Nat. Phys. **1**, 189 (2005).
[3]B.-R. Hyun *et al.*, ACS Nano **2**, 2206 (2008).
[4]K. W. Johnston *et al.*, Appl. Phys. Lett. **92**, 151115 (2008).
[5]R. Bayon *et al.*, C. R. Chim. **9**, 730 (2006).
[6]J. M. Luther *et al.*, Nano Lett. **8**, 3488 (2008).
[7]W. Ma *et al.*, Nano Lett. **9**, 1699 (2009).
[8]J. J. Choi *et al.*, Nano Lett. **9**, 3749 (2009).
[9]K. S. Leschkies *et al.*, ACS Nano **3**, 3638 (2009).
[10]R. Vogel, P. Hoyer, and H. Weller, J. Phys. Chem. **98**, 3183 (1994).
[11]P. Hoyer and R. Konenkamp, Appl. Phys. Lett. **66**, 349 (1995).
[12]R. Plass *et al.*, J. Phys. Chem. B **106**, 7578 (2002).
[13]R. O'Hayre *et al.*, Adv. Funct. Mater. **16**, 1566 (2006).
[14]I. E. Anderson *et al.*, Appl. Phys. Lett. **94**, 063101 (2009).
[15]A. J. Breeze *et al.*, Phys. Rev. B **64**, 125205 (2001).
[16]E. J. D. Klem *et al.*, Appl. Phys. Lett. **90**, 183113 (2007).
[17]H. E. Romero and M. Drndic, Phys. Rev. Lett. **95**, 156801 (2005).
[18]G. Dedigamuwa *et al.*, Appl. Phys. Lett. **95**, 122107 (2009).
[19]R. Loef *et al.*, J. Phys. Chem. C **113**, 15992 (2009).
[20]Y. Liu *et al.*, Nano Lett. **10**, 1960 (2010).
[21]M. H. Zarghami *et al.*, ACS Nano **4**, 2475 (2010).
[22]D. R. Huntley, J. Phys. Chem. **99**, 12907 (1995).

This article is copyrighted as indicated in the article. Reuse of AIP content is subject to the terms at: http://scitation.aip.org/termsconditions. Downloaded to IP: 128.114.130.190 On: Fri, 30 Jan 2015 21:49:13